The International Journal of Cardiovascular Imaging (2019) 35:1767–1776
https://doi.org/10.1007/s10554-019-01636-3

ORIGINAL PAPER

Optical coherence tomography evaluation of the absorb bioresorbable scaffold performance for overlap versus non-overlap segments in patients with coronary chronic total occlusion: insight from the GHOST-CTO registry

Gabriel T. R. Pereira[1,4] · Alessio La Manna[2] · Yasuhiro Ichibori[1] · Armando Vergara-Martel[1] · Bruno Ramos Nascimento[3] · Abdul Jawwad Samdani[1] · Davide Capodanno[2] · Guido D'Agosta[2] · Giacomo Gravina[2] · Giuseppe Venuti[2] · Corrado Tamburino[2] · Guilherme F. Attizzani[1,4]

Received: 17 December 2018 / Accepted: 27 May 2019 / Published online: 7 June 2019

Abstract

The Absorb bioresorbable vascular scaffold (BVS) promised to avoid some of the disadvantages of its metal predecessors. Even though it has been taken off the market, limited data is available about its use in coronary chronic total occlusion (CTO) and its performance in overlap segments, which would be of special research interest due to its large thickness. This data is still pertinent since the platform of bioresorbable devices has not been abandoned, with several companies working on it. We aimed to compare healing and performance between overlap (OL) and non-overlap regions (NOL) of CTO lesions treated with BVS, using optical coherence tomography (OCT). Fourteen patients with overlapping BVS were included from the GHOST-CTO registry, resulting in 25 OL and 38 NOL regions. OCT based parameters were compared between OL and NOL groups at baseline (post-implantation) and 12-month follow-up. The mean age was 61.7 ± 7.2 years and 12 (86%) were males. Twelve (86%) patients underwent PCI for stable coronary artery disease and 2 (14%) had unstable angina. At 12-month follow-up, mean lumen area decreased in both NOL and OL regions, but the decrease was significantly larger in the OL region (NOL −0.7 ± 1.33 vs. OL −2.4 ± 1.54 mm^2; p = 0.002). Mean scaffold area increased in both regions, but increased significantly more in NOL (+1.1 ± 1.54 vs. +0.4 ± 1.16 mm^2; p = 0.016). The percent of uncovered struts was lower in the OL group (5.0 ± 6.6% vs. 3.75 ± 8.7%, p = 0.043), whereas the percentage of malapposed struts was similar (0.3 ± 0.5% vs. 0.7 ± 2.3%, p = 0.441). Neointimal hyperplasia (NIH) was more pronounced in the OL region (0.13 ± 0.04 vs. 0.24 ± 0.10 mm^2, p = 0.001). The OL and NOL segments showed comparable healing in terms of coverage and malapposition. However, NIH was more prominent in OL region. The long-term clinical implications of these findings needs further evaluation. The present study provides important insights for future development of BVS technology.

Keywords BVS · OCT · CTO PCI · Overlap segments · Intravascular imaging

✉ Gabriel T. R. Pereira
gtensolr@gmail.com

✉ Guilherme F. Attizzani
guilherme.attizzani@uhhospitals.org

[1] Case Western Reserve University and Harrington Heart and Vascular Institute, University Hospitals, Cleveland Medical Center, Cleveland, USA

[2] Cardio-Thoracic-Vascular Department, Azienda Ospedaliero-Universitaria "Policlinico-Vittorio Emanuele", University of Catania, Catania, Italy

[3] Hospital das Clínicas, Universidade Federal de Minas Gerais, Belo Horizonte, Brazil

[4] Cardiovascular Imaging Core Laboratory, Harrington Heart & Vascular Institute, University Hospitals Cleveland Medical Center, 11100 Euclid Avenue, Lakeside building, Room 3113, Mailstop Lakeside 5038, Cleveland, OH 44106, USA

Introduction

Percutaneous coronary intervention (PCI) involving chronic total occlusion (CTO) frequently requires the implantation of long and multiple stents, ultimately leading to several overlapping segments. While metallic drug-eluting stents (DES) are commonly used for CTO PCI [1, 2], they have certain inherent disadvantages originating from the permanent nature of metal stents [3]. Some researchers studied the procedural feasibility and outcomes of using everolimus-eluting bioresorbable vascular scaffolds (BVS, Absorb®, Abbott Vascular, Santa Clara, California, USA) in CTO [4–6], given the promise of BVS to potentially overcome some of the disadvantages of metallic stents by restoring vasomotion, enabling positive remodeling, freeing jailed side branches and causing less interference with future surgical revascularization and non-invasive coronary imaging [7, 8]. However, compared to leading DES, clinical trials [9, 10] failed to demonstrate the translation of theoretical advantages of BVS into clinical benefit; believed, in part, due to the thicker struts [11, 12]. Even though BVS has been taken off the market due to safety concerns related mostly to stent thrombosis, limited data is available about its use in coronary chronic total occlusion (CTO) and its performance in overlap regions, which would be of special research interest due to its thickness. In addition to that, the platform of resorbable scaffolds was not abandoned, with several companies still offering such kinds of products or working on the development of new platforms. When comparing CTO lesions to non-CTO lesions, several authors have found significant differences in the healing pattern, with CTO having a higher restenosis rate, believed to be due to the increased vessel injury during PCI procedure [13–18]. To the best of our knowledge, no studies have investigated in detail the vascular response of BVS in overlap versus non-overlap segments in CTO lesions, therefore we utilized optical coherence tomography (OCT) [19, 20], to compare vascular reactions to BVS implantation in overlap (OL) and non-overlap regions (NOL) in CTO lesions.

Material and methods

Population

This is a sub-study from the GHOST-CTO registry, which was a prospective, single center study conducted at the Ferrarotto Hospital, Catania, Italy. Detailed inclusion and exclusion criteria of the GHOST-CTO registry were previously published [4]. An informed, written consent was obtained from all patients. In summary, all patients undergoing PCI of a CTO, between May 2013 and May 2014, were evaluated for BVS implantation after recanalization. For the purpose of this sub-study, patients that had overlapping BVS implantation and had OCT pullbacks available for both baseline (post-PCI) and follow-up (12 month) time-points were included. The following exclusion criteria were applied: (1) reference vessel diameter (RVD) ≤ 2.25 or ≥ 3.8 mm; and (2) target lesion located in a true bifurcation involving a side branch ≥ 2 mm.

PCI procedure

Trans-femoral and trans-radial approaches were used in addition to a variety of techniques (anterograde and retrograde) at the operator's discretion and expertise. After recanalization, pre-dilation was performed using semi-compliant, non-compliant, scoring or cutting balloons as deemed necessary. Post-dilation, when necessary, was achieved using an appropriately sized balloon, not exceeding 0.5 mm of oversizing. The use of intravascular ultrasound (IVUS) guidance was allowed at the discretion of the operator. The BVS scaffolds were overlapped utilizing the marker-to-marker technique, with the intention to minimize the overlap length while not having a gap between scaffolds.

OCT acquisition protocol

Frequency-domain OCT (FD-OCT, Abbott Vascular, Santa Clara, CA, USA) acquisition was performed post BVS implantation and at 12-months with the non-occlusive technique by automatic contrast injection at a flow of 4–6 ml/s. The pullback started distally to the treated segment and continued either until the probe entered into the guiding catheter or the maximum pullback length was reached. If required, additional pullbacks were performed to enable full visualization of the treated segment. Before image acquisition, routine calibration was accomplished by adjusting the Z-offset, either automatically or manually and intracoronary nitrates were administered (100–300 µg according to aortic pressure).

OCT quantitative analysis

OCT analysis was performed using the OPTIS™ Off-line Review Workstation (Version E.4; St. Jude Medical) by 2 independent analysts blinded to patient characteristics and then reviewed by 2 other analysts. All analysts were trained in the Harrington Cardiovascular Imaging Core Laboratory and certified against a gold standard by statistical analysis. All cross-sectional images of the pullbacks were initially screened for quality assessment and excluded if: (1) part of the image was out-of-screen; (2)

a side branch occupied more than 45°; or (3) the quality of the images was poor due to residual blood or artifacts. All the pullbacks had the Z-offset calibration checked and corrected before the analysis. Quantitative analysis was performed every 0.6 mm in the NOL segments [21], and every 0.2 mm in the OL segments. The BVS was analyzed using both adluminal and abluminal interpolated contours, however, for the purpose of this substudy, only abluminal parameters are reported. Malapposition was considered when there was no contact, at any point, between the scaffold and vessel [22]. The quantitative analysis included common measures like minimum, mean and maximum areas of scaffold and lumen. In overlapping regions, the outer scaffold was used for tracing, while all scaffolds struts were analyzed (inner and outer scaffold) for coverage and malapposition.

Clinical outcomes and definitions

Acute technical success was defined as successful scaffold delivery and deployment at the target lesion, after CTO recanalization, with attainment of a final residual stenosis < 30% within the treated segment and restoration of TIMI 3 antegrade flow in the target vessel. Procedural success was defined as technical success in the absence of major adverse cardiac events (MACE) during hospital stay. MACE were assessed at 1 year and defined as a composite of death, myocardial infarction (MI) and target lesion revascularization (TLR). Death was considered of cardiac nature if any other obvious causes were not recognized, in keeping with the Academic Research Consortium [23].

Statistical analysis

Categorical variables are presented as numbers and percentages. Continuous variables are presented as means and standard deviations or medians and interquartile ranges, when appropriate. All analyses were performed in SPSS version 20 using the Wilcoxon Signed Rank test. OCT-based variables were compared between OL and NOL regions at both baseline and follow-up, and where applicable, delta changes are compared. A p-value < 0.05 was considered to indicate statistical significance.

Results

A total of 14 patients from the GHOST-CTO registry that fulfilled the inclusion criteria were included in the present study.

Table 1 Demographic, clinical, lesion and procedural characteristics

Variable	*n* = 14
Age, years, mean (SD)	61.7 (7.2)
Male, n (%)	12 (85.71)
Risk factors	
Hypertension, n (%)	11 (78.57)
Dyslipidemia, n (%)	10 (71.42)
Smoker, n (%)	5 (35.71)
Previous smoker, n (%)	6 (42.86)
Diabetes, n (%)	5 (35.71)
Family history, n (%)	5 (35.71)
BMI, kg/m^2, mean (SD)	27.90 (4.31)
BMI ≥ 30 kg/m^2, n (%)	6 (42.86)
Medical history	
Previous PCI, n (%)	9 (64.29)
Previous CABG, n (%)	0
Previous stroke/TIA, n (%)	1 (7.14)
LVEF, %, mean (SD)	51.50 (8.77)
Basal GFR, mean (SD)	112.78 (37.96)
Clinical presentation	
Stable angina, n (%)	12 (85.71)
Unstable angina, n (%)	2 (14.29)
Myocardial infarction, n (%)	0
Asymptomatic, n (%)	0
Target CTO lesion	
LMCA, n (%)	0
LAD, n (%)	4 (28.57)
LCx, n (%)	4 (28.57)
RCA, n (%)	6 (42.86)
SYNTAX score, mean (SD)	14.20 (7.75)
Lesion information and preparation	
Pre-dilation, n (%)	14 (100)
Calcium score, mean (SD)	1.43 (0.94)
Noncompliant balloon, n (%)	6 (33.3)
Scoring/cutting balloon, n (%)	3 (21.43)
Rotational atherectomy, n (%)	0
Post-dilatation, n (%)	14 (100)
Max post-dilation pressure, atm, mean (SD)	17.57 (3.61)
Post-dilation balloon diameter, mm, mean (SD)	3.5 (0.33)
Post-dilations performed per case, mean (SD)	2.57 (1.16)
Post-dilation of overlapping segment, n (%)	14 (100)
Post-dilation of non-overlapping segment, n (%)	14 (100)
Scaffolds per case, mean (SD)	3.29 (1.2)
Scaffold length, mm, mean (SD)	23.78 (5.78)
Scaffold diameter, mm, mean (SD)	3.18 (0.36)
Technical success, n (%)	13 (92.86)
Procedural success, n (%)	13 (92.86)

BMI body mass index, *PCI* percutaneous coronary intervention, *CABG* coronary artery by-pass, *TIA* transient ischemic attack, *LVEF* left ventricle ejection fraction, *GFR* glomerular filtration rate, *LMCA* left main coronary artery, *LAD* left anterior descending artery, *LCx* Left circumflex artery, *RCA* right coronary artery

Patient population, lesion characteristics and procedural parameters

Demographic, clinical, lesion and procedural characteristics are summarized in Table 1. Mean age was 61.7 ± 7.2 years and 12 (85.71%) patients were male. Twelve (85.71%) patients had stable angina at the time of the index procedure and 2 (14.29%) presented with unstable angina. The most common cardiovascular risk factor was hypertension 11 (78.57%) followed by dyslipidemia 10 (71.42%), obesity 6 (42.86%), diabetes mellitus 5 (35.71%), active tobacco use 5 (35.71%) and family history 5 (35.71%). Mean LVEF was 51.5% ± 8.8%.

In terms of CTO target vessel distribution, the right coronary artery 6 (42.86%) was the most common, followed equally by left anterior descending and left circumflex arteries 4 (28.6% each). Mean SYNTAX-1 score was 14.2 ± 7.8. Most lesions had mild calcification, with one lesion having a calcium score of 3 and none with a calcium score of 4, as assessed by OCT, with a mean score of 1.43 [24]. Post-dilatation was performed in all patients (100%) with mean maximum post dilation pressure of 17.6 ± 3.6 atm. When comparing post dilation by segments, all of the 14 patients (100%) had post dilation performed at both the overlapping and non-overlapping segments. The average post dilation balloon diameter was 3.5 ± 0.33 mm and the average post dilation inflation number per patient was 2.57 ± 1.16. Technical success was obtained in 13 (92.86%) patients. One patient had technical failure because of residual stenosis above 30%. There were no MACE during the hospital stay, corresponding to a procedural success of 13 (92.86%).

OCT results

There were 38 NOL regions and 25 OL regions that were analyzed and compared. At baseline (post-PCI), a total of 1297 frames (11,219 struts) were analyzed in the NOL segments and 323 frames (2820 struts) in the OL regions. At 12-month follow-up time-point, the number of frames (struts) analyzed in the NOL and OL segments was 1371 (11,304) and 315 (2789) respectively.

Comparison of OCT outcomes between OL and NOL regions at baseline and follow-up are shown in Table 2 and the deltas between FU to BL in the Graphic 1. The mean lumen area was smaller in the NOL region at baseline (8.11 ± 1.83 vs. 8.69 ± 1.91 mm^2; p = 0.023) and it decreased in both regions at 12-month follow-up. However, compared to the NOL, there was a larger decrease in the OL region (NOL − 0.71 ± 1.33 vs. OL − 2.38 ± 1.54 mm^2; p = 0.002), resulting in larger lumen area in NOL region at follow-up. The minimum lumen area was significantly smaller in the NOL compared to OL both at baseline (5.45 ± 1.99 vs. 7.48 ± 2.04 mm^2; p = 0.001) and at follow-up (3.66 ± 1.49 vs. 5.38 ± 1.76 mm^2; p = 0.001). In both groups, it decreased at the follow up and the delta was not different (− 1.79 ± 131 vs. − 2.10 ± 1.62 mm^2; p = 0.272). The maximum lumen area was significantly larger in the NOL region at baseline

Table 2 Optical coherence tomography findings at baseline and follow-up

Variable	NOL (n = 14)	OL (n = 14)	p Value
Minimum lumen area			
BL, mm^2 (SD)	5.45 (1.99)	7.48 (2.04)	**0.013**
FU, mm^2 (SD)	3.66 (1.49)	5.38 (1.76)	**0.010**
Maximum lumen area			
BL, mm^2 (SD)	11.22 (2.18)	9.67 (2.04)	0.062
FU, mm^2 (SD)	13.08 (4.01)	7.90 (2.25)	**0.000**
Mean lumen area			
BL, mm^2 (SD)	8.11 (1.83)	8.69 (1.91)	0.419
FU, mm^2 (SD)	7.40 (1.79)	6.31 (1.72)	0.113
Mean lumen diameter			
BL, mm (SD)	3.16 (0.38)	3.29 (0.37)	0.382
FU, mm (SD)	2.99 (0.38)	2.79 (0.40)	0.184
Minimum scaffold ablumi-nal area			
BL, mm^2 (SD)	5.78 (2.11)	7.93 (1.96)	**0.010**
FU, mm^2 (SD)	5.65 (1.54)	8.47 (1.93)	**0.000**
Maximum scaffold ablumi-nal area			
BL, mm^2 (SD)	11.62 (2.12)	10.52 (1.97)	0.164
FU, mm^2 (SD)	16.28 (4.84)	11.18 (2.93)	**0.003**
Mean scaffold abluminal area			
BL, mm^2 (SD)	8.65 (1.89)	9.39 (1.81)	0.298
FU, mm^2 (SD)	9.77 (2.13)	9.77 (2.16)	0.993
Mean scaffold abluminal diameter			
BL, mm (SD)	3.27 (0.38)	3.43 (0.33)	0.267
FU, mm (SD)	3.46 (0.39)	3.49 (0.40)	0.845
Embedded struts (BL)			
% (SD)	9.52 (10.15)	14.35 (17.78)	0.387
Covered struts (FU)			
% (SD)	95.00 (6.58)	96.25 (8.73)	0.674
Malapposed struts			
BL, % (SD)	4.62 (4.99)	5.79 (4.87)	0.536
FU, % (SD)	0.29 (0.46)	0.69 (2.32)	0.538
Mean malapposition area			
BL, mm^2 (SD)	0.26 (0.20)	0.25 (0.19)	0.831
FU, mm^2 (SD)	0.07 (0.07)	0.02 (0.03)	**0.022**
Mean plaque protruding area (BL)			
mm^2 (SD)	0.08 (0.07)	0.14 (0.16)	0.183
Neointimal hyperplasia (FU)			
mm^2 (SD)	0.13 (0.04)	0.24 (0.1)	**0.007**

Bold numbers indicate p-value < 0.05, to demonstrate statisticaly significance

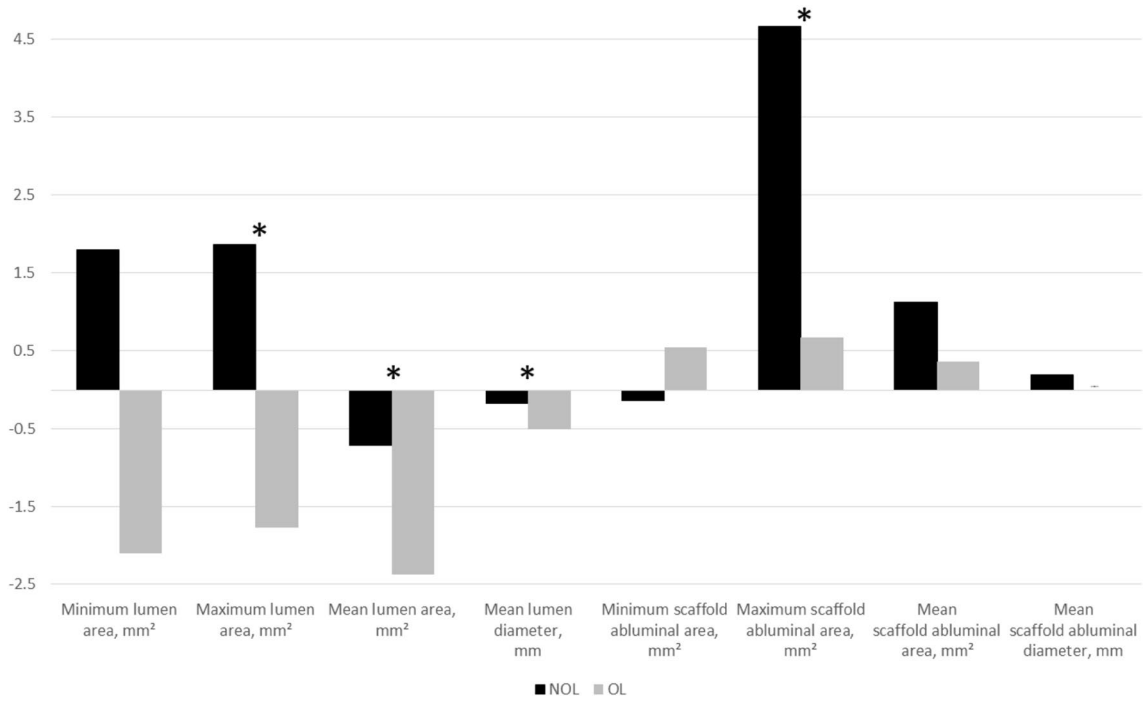

Graphic 1 Delta of optical coherence tomography measurements from follow-up to baseline comparing NOL and OL regions. NOL: Non-overlap regions; OL: Overlap regions; Asterisk (*): indicates statistical significance

(11.22 ± 2.18 vs. 9.67 ± 2.04 mm^2; $p = 0.005$). At follow-up, it increased ($+1.86 \pm 3.17$ mm^2) in the NOL segments and decreased (-1.77 ± 1.63 mm^2) in the OL regions, with a significant difference in the delta ($p = 0.001$).

The mean (abluminal) scaffold area was smaller in NOL segments at baseline (8.65 ± 1.89 vs. 9.39 ± 1.81 mm^2; $p = 0.004$). At follow-up, it increased in both regions and were similar in comparison (9.77 ± 2.13 vs. 9.77 ± 2.16 mm^2; $p = 0.950$), although the delta was larger in the NOL group ($+1.12 \pm 1.54$ vs. $+0.37 \pm 1.16$ mm^2; $p = 0.016$). As is seen in terms of the minimum lumen area, the minimum scaffold area was also significantly smaller in the NOL compared to OL both at baseline and at follow-up. From baseline to follow-up, a decrease was observed in the NOL (-0.13 ± 1.40 mm^2) contrasting with an increase in the OL segments ($+0.54 \pm 1.47$ mm^2) with similar deltas, however ($p = 0.158$). In terms of maximum scaffold area, it was larger in the NOL group at baseline (11.62 ± 2.12 vs. 10.52 ± 1.97 mm^2; $p = 0.022$). It increased in both groups, but the increase was significantly larger in the NOL region ($+4.66 \pm 4.00$ vs. $+0.67 \pm 1.65$ mm^2; $p = 0.004$).

After scaffold placement, the percentage of embedded struts and malapposed struts as well as the mean plaque protrusion area showed no difference between NOL and OL regions (Table 2). In terms of healing at follow-up, the percentage of covered struts was higher in OL regions (NOL 95.0 ± 6.58 vs. OL 96.25 ± 8.73%, $p = 0.043$), but the percentage of malapposed struts was similar between the groups (0.29 ± 0.76 vs. 0.69 ± 2.32%, $p = 0.441$). Of note, malapposition (in terms of percentage of malapposed struts) decreased in both groups and the difference in delta percent was not significant (-4.33 ± 5.05% vs. -5.10 ± 4.44%; $p = 0.433$). However, neointimal hyperplasia (NIH) was more pronounced in the OL region (NOL 0.13 ± 0.04 mm^2 vs. OL 0.24 ± 0.10 mm^2, $p = 0.001$).

Clinical outcomes

The mean follow-up duration was 385.25 ± 36.10 days. There were no MACE (death, myocardial infarction or target vessel revascularization) noted during the follow-up period.

Discussion

When comparing OL to NOL segments in CTO lesions treated with overlapping BVS at 12 months, we observed that (1) despite a similar mean scaffold area, the lumen area was smaller in OL group, resulting from a significantly larger lumen loss in OL group from baseline to follow up, (2) percentage of uncovered struts was low in both groups but interestingly lower in the OL group, (3) percentage of malapposed struts was comparable and very low in both the NOL and OL segments, suggesting an acceptable healing

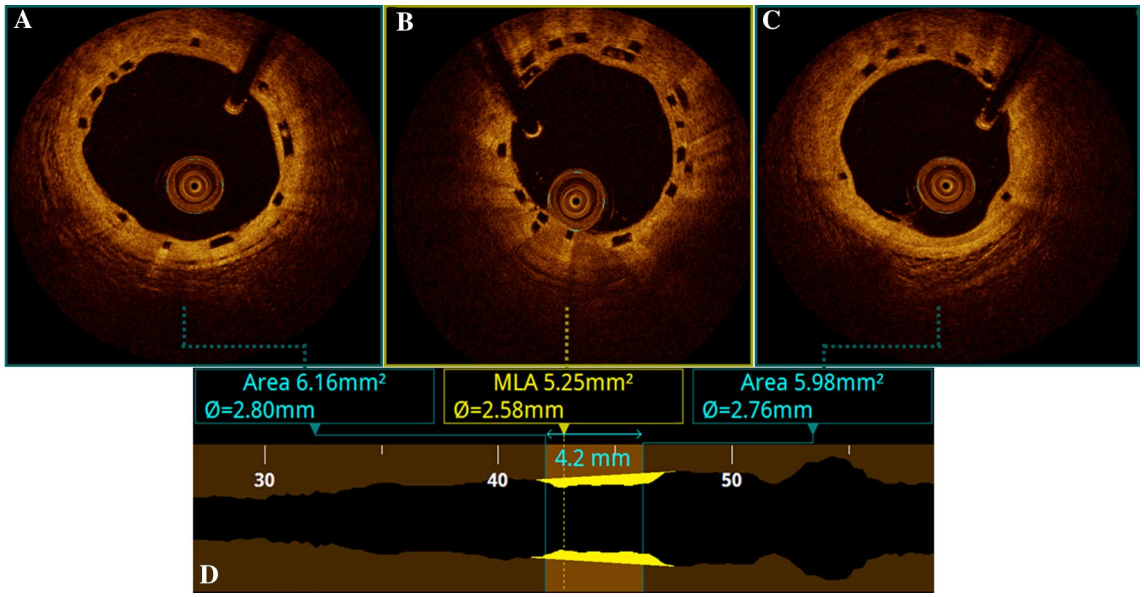

Fig. 1 Representative OCT cross section with lumen profile comparison between NOL and OL regions follow-up: OCT cross sectional images and lumen profile view at follow-up comparing OL and NOL regions. **a** and **c** represent distal and proximal images adjacent to the overlapping segment (**b**). Image **d** shows measurements in these regions, indicating a smaller lumen on the OL region, when comparing to the NOL segments, as represented in yellow. NOL: non-overlap, OCT: optical coherence tomography, OL: overlap

pattern, and (4) NIH area was significantly larger in OL segments.

The larger lumen loss in OL regions is explained by the more pronounced NIH area (as represented by Fig. 1) and restriction of positive remodeling in OL segment by two layers of struts. Our finding of larger NIH in overlap segments is consistent with a previous study by Sato et al. that examined neointimal coverage of overlapping bioresorbable scaffolds [25]. Studies on DES have also shown exaggerated and heterogenous neointimal reactions in overlap regions [26, 27]. A deeper examination of the phenomenon of thicker NIH in OL region in our study revealed that the inner scaffold acted as a bridge for the neo-intimal growth as represented by Fig. 2. This idea is supported by the Porcine Coronary Artery Model [28], with a similar conclusion: the thicker NIH in OL regions is mostly driven by the stacked struts. In keeping with the protocol set forth in consensus guidelines [29, 30], we measured the NIH from the outer scaffold to the lumen in the OL segments. Perhaps, it can be appreciated by visual evaluation of Figs. 1 and 2, that the neointimal growth over the inner scaffold struts in the OL segments is similar to the NIH in the NOL region (Fig. 3).

It is also noteworthy that even though the mean scaffold areas were similar at follow-up between NOL and OL regions, the scaffold area increased in both groups compared to the baseline. This finding is consistent with the phenomenon of positive remodeling as described previously [7, 8]. However, we observed that the increase in scaffold area from post-implantation to follow-up was more pronounced in the NOL segments, reflecting that positive remodeling and vasomotion are possibly restricted by the two layers of scaffold [31] and increased material burden at the OL site.

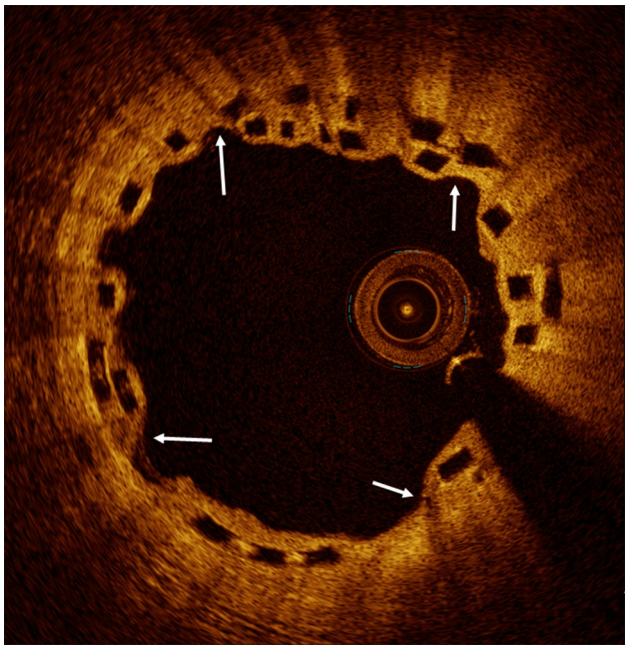

Fig. 2 OCT cross section with overlapping scaffolds: White arrows indicate regions where the inner scaffold acts as a bridge for the NIH growth. NIH: neointima hyperplasia, OCT: optical coherence tomography

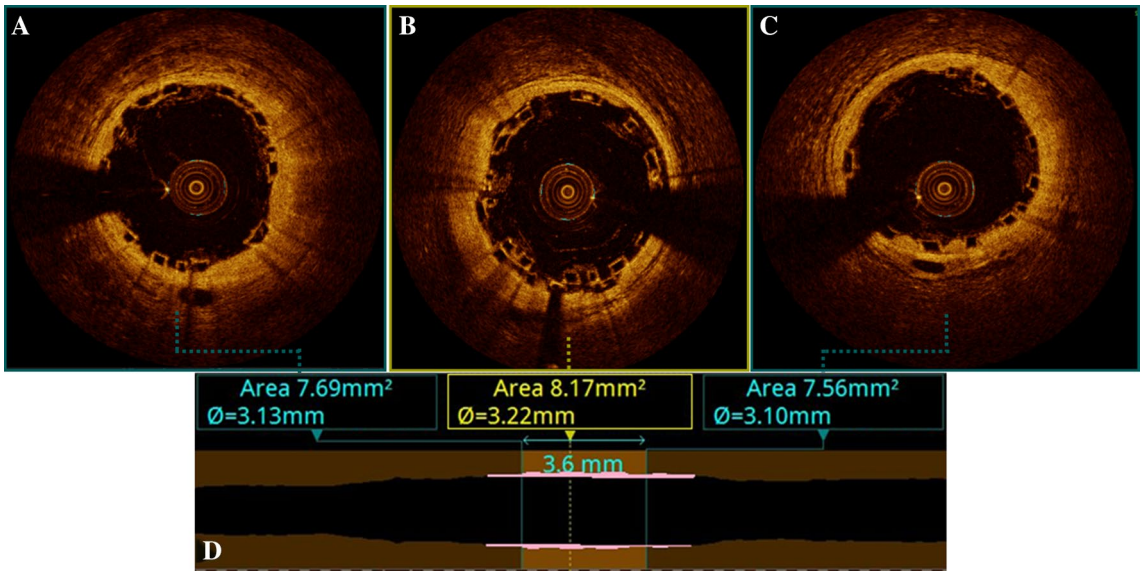

Fig. 3 Representative OCT cross section with lumen profile comparison between NOL and OL regions at baseline: OCT cross sectional images and lumen profile view at baseline, comparing OL and NOL regions. **a** and **c** represent distal and proximal images adjacent to the overlapping segment (**b**). Image **d** shows the measurements in those regions, indicating a bigger lumen on the OL regions, when comparing to the NOL segments, as represented by the area in red. NOL: non-overlap, OCT: optical coherence tomography, OL: overlap

At baseline, we saw larger mean lumen and scaffold areas (Fig. 2) in the OL compared to NOL region as well as a trend towards larger mean plaque protruding area and percentage of embedded struts. These findings may be explained by a more thorough implantation of overlapping scaffolds and more aggressive post dilation in the OL regions resulting in better expansion. We did not have specific data/procedural details to examine and confirm this concept.

Our data shows that the minimum lumen and scaffold areas in the OL segments were larger than the NOL segments but the maximum lumen and scaffold areas were smaller in the OL segments compared to the NOL. These findings may be explained by the fact that the NOL segments represent the whole length of the target CTO lesion including the smaller distal and larger proximal segments than the OL regions that lied in between.

The impact of endothelial shear stress (EES) on neointimal proliferation following BMS and DES implantation has been explored, and more recently, a serial OCT study of BVS implantation has shown an inverse association between ESS and neointimal thickness [32–35]. Additionally, stent design has shown to impact flow characteristics; importantly showing stent strut size-dependent decreases in downstream ESS [36]. Moreover, the relative configuration of stent struts (congruent vs. non-congruent) has shown to further impact downstream ESS, with congruent (stacked) struts resulting in lower near-wall velocities and decreased ESS [37]. Given the principle of our study, we would expect both the larger nature of BVS struts and the interplay between overlapping stents to impact neointimal development in the microenvironment and should be the focus of a future study using computational fluid dynamics and OCT strut-level analysis. We can hypothesize that similar to DES, the BVS strut's congruent and non-congruent configurations would result in flow disturbances with congruent struts resulting in greater decrease in downstream ESS, but studies must be conducted.

This study utilizing OCT further supports the results from other groups that evaluated the safety, feasibility [38], clinical [6, 39–41] and intravascular imaging outcomes [25, 28, 38] of overlapping BVS, showing that despite having some key differences to non-overlap segments, it was not associated with cardiac death, target lesion revascularization and stent thrombosis despite a higher incidence of peri-procedural MI found in ABSORB EXTEND [39].

Although ABSORB BVS has been removed from the market due to safety concerns [42], we believe that our study, by providing important insight into BVS performance in a specific use related to overlap in CTO lesions, can help in future development of BVS technology and can be extrapolated to other stents. The acceptable healing pattern observed suggests that this technology may be further developed and tested in future platforms, even in high-complexity angiographic scenarios.

Limitations

The analysis presented in this study was performed from a nonrandomized, single center study having the possibility of selection and procedure bias, and the study also applies

to a CTO population with intermediate to high complexity. Secondly, the sample size was small, however, we analyzed multiple OL and NOL segments and a very high number of frames and struts to strengthen the data. In addition the study observation time is short and underpowered for low-frequency events like stent failure, and also for any conclusions about clinical outcomes. Nonetheless, it is the first study to evaluate overlapping BVS on CTO lesions using clinical and imaging endpoints, shedding light for future studies and observations in the CTO field.

Conclusion

The overlap and non-overlap segments showed comparable healing pattern in terms of high coverage and low malapposition at 12-month follow-up OCT imaging. However, NIH was more prominent in OL region; resulting in larger lumen loss compared to NOL region. The long-term clinical implications of these findings need further study. The study provides important insight for future development of BVS technology.

Compliance with ethical standards

Conflict of interest Guilherme F. Attizzani - Speaker for Abbott, Alessio La Manna - Consultant for Abbott. The other authors have no conflicts of interest to disclose.

References

1. De Felice F, Fiorilli R, Parma A, Nazzaro M, Musto C, Sbraga F, Caferri G, Violini R (2009) Year clinical outcome of patients with chronic total occlusion treated with drug-eluting stents. JACC 2(12):1260–1265. https://doi.org/10.1016/j.jcin.2009.09.013
2. Mori H, Lutter C, Yahagi K, Harari E, Kutys R, Fowler DR, Ladich E, Joner M, Virmani R, Finn AV (2017) Pathology of chronic total occlusion in bare-metal versus drug-eluting stents: implications for revascularization. JACC Cardiovasc Interv 10(4):367–378. https://doi.org/10.1016/j.jcin.2016.11.005
3. Nakamura D, Attizzani GF, Toma C, Sheth T, Wang W, Soud M, Aoun R, Tummala R, Leygerman M, Fares A, Mehanna E, Nishino S, Fung A, Costa MA, Bezerra HG (2016) Failure mechanisms and neoatherosclerosis patterns in very late drug-eluting and bare-metal stent thrombosis. Circulation 9(9):003785. https://doi.org/10.1161/circinterventions.116.003785
4. La Manna A, Chisari A, Giacchi G, Capodanno D, Longo G, Di Silvestro M, Capranzano P, Tamburino C (2016) Everolimus-eluting bioresorbable vascular scaffolds versus second generation drug-eluting stents for percutaneous treatment of chronic total coronary occlusions: Technical and procedural outcomes from the GHOST-CTO registry. Catheter Cardiovasc Interv 88(6):E155–E163. https://doi.org/10.1002/ccd.26397
5. Manna A, Micciché E, D'Agosta G, Tensol Rodrigues Pereira G, Attizzani GF, Capranzano P, Capodanno D, Tamburino C (2017) Vascular response and healing profile of everolimus-eluting bioresorbable vascular scaffolds for percutaneous treatment of chronic total coronary occlusions: a one-year optical coherence tomography analysis from the GHOST-CTO registry. Int J Cardiol 1:1. https://doi.org/10.1016/j.ijcard.2017.10.107
6. Vaquerizo B, Barros A, Pujadas S, Bajo E, Estrada D, Miranda-Guardiola F, Rigla J, Jiménez M, Cinca J, Serra A (2015) Bioresorbable everolimus-eluting vascular scaffold for the treatment of chronic total occlusions: CTO-ABSORB pilot study. EuroIntervention 11(5):555–563. https://doi.org/10.4244/eijy14m12_07
7. Onuma Y, Ormiston J, Serruys PW (2011) Bioresorbable Scaffold technologies. Circ J 75(3):509–520. https://doi.org/10.1253/circj.cj-10-1135
8. Serruys PW, Garcia-Garcia HM, Onuma Y (2011) From metallic cages to transient bioresorbable scaffolds: change in paradigm of coronary revascularization in the upcoming decade? Eur Heart J 33(1):16–25. https://doi.org/10.1093/eurheartj/ehr384
9. Ali ZA, Gao RF, Kimura T, Onuma Y, Kereiakes DJ, Ellis SG, Chevalier B, Vu M-T, Zhang Z, Simonton CA, Serruys PW, Stone GW (2017) Three-year outcomes with the absorb bioresorbable scaffold: individual-patient-data meta-analysis from the ABSORB randomized trials. Circulation. https://doi.org/10.1161/circulationaha.117.031843
10. Kereiakes DJ, Ellis SG, Metzger C, Caputo RP, Rizik DG, Teirstein PS, Litt MR, Kini A, Kabour A, Marx SO, Popma JJ, McGreevy R, Zhang Z, Simonton C, Stone GW (2017) 3-year clinical outcomes with everolimus-eluting bioresorbable coronary scaffolds. J Am Coll Cardiol 70(23):2852–2862. https://doi.org/10.1016/j.jacc.2017.10.010
11. Kastrati A, Mehilli J, Dirschinger J, Dotzer F, Schuhlen H, Neumann FJ, Fleckenstein M, Pfafferott C, Seyfarth M, Schomig A (2001) Intracoronary stenting and angiographic results: strut thickness effect on restenosis outcome (ISAR-STEREO) trial. Circulation 103(23):2816–2821. https://doi.org/10.1161/01.cir.103.23.2816
12. Kawamoto H, Jabbour RJ, Tanaka A, Latib A, Colombo A (2016) The Bioresorbable Scaffold. JACC 9(3):299–300. https://doi.org/10.1016/j.jcin.2015.11.019
13. Michael TT, Mogabgab O, Alomar M, Kotsia A, Christopoulos G, Rangan BV, Abdullah S, Grodin J, Banerjee S, Brilakis ES (2014) Long-term outcomes of successful chronic total occlusion percutaneous coronary interventions using the antegrade and retrograde approach. J Interv Cardiol 27(5):465–471. https://doi.org/10.1111/joic.12149
14. George S, Cockburn J, Clayton TC, Ludman P, Cotton J, Spratt J, Redwood S, de Belder M, de Belder A, Hill J, Hoye A, Palmer N, Rathore S, Gershlick A, Di Mario C, Hildick-Smith D, British CardiovascularIntervention S, National Institute for Cardiovascular Outcomes R (2014) Long-term follow-up of elective chronic total coronary occlusion angioplasty: analysis from the U.K. Central cardiac audit database. J Am Coll Cardiol 64(3):235–243. https://doi.org/10.1016/j.jacc.2014.04.040
15. Valenti R, Vergara R, Migliorini A, Parodi G, Carrabba N, Cerisano G, Dovellini EV, Antoniucci D (2013) Predictors of reocclusion after successful drug-eluting stent-supported percutaneous coronary intervention of chronic total occlusion. J Am Coll Cardiol 61(5):545–550. https://doi.org/10.1016/j.jacc.2012.10.036
16. Garcia S, Abdullah S, Banerjee S, Brilakis ES (2013) Chronic total occlusions: patient selection and overview of advanced techniques. Curr Cardiol Rep 15(2):334. https://doi.org/10.1007/s11886-012-0334-2
17. Brilakis ES, Kotsia A, Luna M, Garcia S, Abdullah SM, Banerjee S (2013) The role of drug-eluting stents for the treatment of coronary chronic total occlusions. Expert Rev Cardiovasc Ther 11(10):1349–1358. https://doi.org/10.1586/14779072.2013.838142

18. Matsumoto D, Shite J, Shinke T, Otake H, Tanino Y, Ogasawara D, Sawada T, Paredes OL, Hirata K, Yokoyama M (2007) Neointimal coverage of sirolimus-eluting stents at 6-month follow-up: evaluated by optical coherence tomography. Eur Heart J 28(8):961–967. https://doi.org/10.1093/eurheartj/ehl413
19. Bezerra HG, Attizzani GF, Sirbu V, Musumeci G, Lortkipanidze N, Fujino Y, Wang W, Nakamura S, Erglis A, Guagliumi G, Costa MA (2013) Optical coherence tomography versus intravascular ultrasound to evaluate coronary artery disease and percutaneous coronary intervention. JACC 6(3):228–236. https://doi.org/10.1016/j.jcin.2012.09.017
20. Bezerra HG, Costa MA, Guagliumi G, Rollins AM, Simon DI (2009) Intracoronary optical coherence tomography: a comprehensive review clinical and research applications. JACC Cardiovasc Interv 2(11):1035–1046. https://doi.org/10.1016/j.jcin.2009.06.019
21. Mehanna EA, Attizzani GF, Kyono H, Hake M, Bezerra HG (2011) Assessment of coronary stent by optical coherence tomography, methodology and definitions. Int J Cardiovasc Imaging 27(2):259–269. https://doi.org/10.1007/s10554-010-9793-y
22. Nakatani S, Sotomi Y, Ishibashi Y, Grundeken MJ, Tateishi H, Tenekecioglu E, Zeng Y, Suwannasom P, Regar E, Radu MD, Raber L, Bezerra H, Costa MA, Fitzgerald P, Prati F, Costa RA, Dijkstra J, Kimura T, Kozuma K, Tanabe K, Akasaka T, Di Mario C, Serruys PW, Onuma Y (2016) Comparative analysis method of permanent metallic stents (XIENCE) and bioresorbable poly-L-lactic (PLLA) scaffolds (Absorb) on optical coherence tomography at baseline and follow-up. EuroIntervention 12(12):1498–1509. https://doi.org/10.4244/EIJY15M10_03
23. Cutlip DE, Windecker S, Mehran R, Boam A, Cohen DJ, van Es GA, Gabriel Steg P, Ma Morel, Mauri L, Vranckx P, McFadden E, Lansky A, Hamon M, Krucoff MW, Serruys PW (2007) Clinical end points in coronary stent trials: a case for standardized definitions. Circulation 115(17):2344–2351. https://doi.org/10.1161/circulationaha.106.685313
24. Fujino A, Mintz GS, Matsumura M, Lee T, Kim SY, Hoshino M, Usui E, Yonetsu T, Haag ES, Shlofmitz RA, Kakuta T, Maehara A (2018) A new optical coherence tomography-based calcium scoring system to predict stent underexpansion. EuroIntervention 13(18):e2182–e2189. https://doi.org/10.4244/EIJ-D-17-00962
25. Sato T, Jose J, El-Mawardy M, Sulimov DS, Tölg R, Richardt G, Abdel-Wahab M (2016) Neointimal coverage of overlapping everolimus-eluting bioresorbable scaffolds: an optical coherence tomography study in native coronary arteries. Int J Cardiol 221:243–245. https://doi.org/10.1016/j.ijcard.2016.07.013
26. Guagliumi G, Musumeci G, Sirbu V, Bezerra HG, Suzuki N, Fiocca L, Matiashvili A, Lortkipanidze N, Trivisonno A, Valsecchi O, Biondi-Zoccai G, Costa MA, Investigators OT (2010) Optical coherence tomography assessment of in vivo vascular response after implantation of overlapping bare-metal and drug-eluting stents. JACC Cardiovasc Interv 3(5):531–539. https://doi.org/10.1016/j.jcin.2010.02.008
27. Gutierrez-Chico JL, Raber L, Regar E, Okamura T, di Mario C, van Es GA, Windecker S, Serruys PW (2013) Tissue coverage and neointimal hyperplasia in overlap versus nonoverlap segments of drug-eluting stents 9 to 13 months after implantation: in vivo assessment with optical coherence tomography. Am Heart J 166(1):83–94. https://doi.org/10.1016/j.ahj.2013.04.001
28. Farooq V, Serruys PW, Heo JH, Gogas BD, Onuma Y, Perkins LE, Diletti R, Radu MD, Räber L, Bourantas CV, Zhang Y, van Remortel E, Pawar R, Rapoza RJ, Powers JC, van Beusekom HMM, Garcìa-Garcìa HM, Virmani R (2013) Intracoronary optical coherence tomography and histology of overlapping everolimus-eluting bioresorbable vascular scaffolds in a porcine coronary artery model. JACC 6(5):523–532. https://doi.org/10.1016/j.jcin.2012.12.131
29. Tearney GJ, Regar E, Akasaka T, Adriaenssens T, Barlis P, Bezerra HG, Bouma B, Bruining N, Cho JM, Chowdhary S, Costa MA, de Silva R, Dijkstra J, Di Mario C, Dudek D, Falk E, Feldman MD, Fitzgerald P, Garcia-Garcia HM, Gonzalo N, Granada JF, Guagliumi G, Holm NR, Honda Y, Ikeno F, Kawasaki M, Kochman J, Koltowski L, Kubo T, Kume T, Kyono H, Lam CC, Lamouche G, Lee DP, Leon MB, Maehara A, Manfrini O, Mintz GS, Mizuno K, Morel MA, Nadkarni S, Okura H, Otake H, Pietrasik A, Prati F, Raber L, Radu MD, Rieber J, Riga M, Rollins A, Rosenberg M, Sirbu V, Serruys PW, Shimada K, Shinke T, Shite J, Siegel E, Sonoda S, Suter M, Takarada S, Tanaka A, Terashima M, Thim T, Uemura S, Ughi GJ, van Beusekom HM, van der Steen AF, van Es GA, van Soest G, Virmani R, Waxman S, Weissman NJ, Weisz G, International Working Group for Intravascular Optical Coherence T (2012) Consensus standards for acquisition, measurement, and reporting of intravascular optical coherence tomography studies: a report from the International Working Group for Intravascular Optical Coherence Tomography Standardization and Validation. J Am Coll Cardiol 59(12):1058–1072. https://doi.org/10.1016/j.jacc.2011.09.079
30. Prati F, Guagliumi G, Mintz GS, Costa M, Regar E, Akasaka T, Barlis P, Tearney GJ, Jang IK, Arbustini E, Bezerra HG, Ozaki Y, Bruining N, Dudek D, Radu M, Erglis A, Motreff P, Alfonso F, Toutouzas K, Gonzalo N, Tamburino C, Adriaenssens T, Pinto F, Serruys PW, Di Mario C, Expert's OCTRD (2012) Expert review document part 2: methodology, terminology and clinical applications of optical coherence tomography for the assessment of interventional procedures. Eur Heart J 33(20):2513–2520. https://doi.org/10.1093/eurheartj/ehs095
31. Rikhtegar F, Wyss C, Stok KS, Poulikakos D, Müller R, Kurtcuoglu V (2014) Hemodynamics in coronary arteries with overlapping stents. J Biomech 47(2):505–511. https://doi.org/10.1016/j.jbiomech.2013.10.048
32. Bourantas CV, Papafaklis MI, Kotsia A, Farooq V, Muramatsu T, Gomez-Lara J, Zhang YJ, Iqbal J, Kalatzis FG, Naka KK, Fotiadis DI, Dorange C, Wang J, Rapoza R, Garcia-Garcia HM, Onuma Y, Michalis LK, Serruys PW (2014) Effect of the endothelial shear stress patterns on neointimal proliferation following drug-eluting bioresorbable vascular scaffold implantation: an optical coherence tomography study. JACC Cardiovasc Interv 7(3):315–324. https://doi.org/10.1016/j.jcin.2013.05.034
33. Papafaklis MI, Bourantas CV, Theodorakis PE, Katsouras CS, Naka KK, Fotiadis DI, Michalis LK (2010) The effect of shear stress on neointimal response following sirolimus- and paclitaxel-eluting stent implantation compared with bare-metal stents in humans. JACC Cardiovasc Interv 3(11):1181–1189. https://doi.org/10.1016/j.jcin.2010.08.018
34. Suzuki N, Nanda H, Angiolillo DJ, Bezerra H, Sabate M, Jimenez-Quevedo P, Alfonso F, Macaya C, Bass TA, Ilegbusi OJ, Costa MA (2008) Assessment of potential relationship between wall shear stress and arterial wall response after bare metal stent and sirolimus-eluting stent implantation in patients with diabetes mellitus. Int J Cardiovasc Imaging 24(4):357–364. https://doi.org/10.1007/s10554-007-9274-0
35. Wentzel JJ, Krams R, Schuurbiers JCH, Oomen JA, Kloet J, Giessen WJVD, Serruys PW, Slager CJ (2001) Relationship between neointimal thickness and shear stress after wallstent implantation in human coronary arteries. Circulation 103(13):1740–1745. https://doi.org/10.1161/01.CIR.103.13.1740
36. Jimenez JM, Davies PF (2009) Hemodynamically driven stent strut design. Ann Biomed Eng 37(8):1483–1494. https://doi.org/10.1007/s10439-009-9719-9
37. Rikhtegar F, Wyss C, Stok KS, Poulikakos D, Muller R, Kurtcuoglu V (2014) Hemodynamics in coronary arteries with overlapping stents. J Biomech 47(2):505–511. https://doi.org/10.1016/j.jbiomech.2013.10.048

38. Farooq V, Onuma Y, Radu M, Okamura T, Gomez-Lara J, Brugaletta S, Gogas B, van Geuns R-J, Regar E, Schultz C, Windecker S, Lefèvre T, Brueren BRG, Powers J, Perkins LL, Rapoza RJ, Virmani R, García-García HM, Serruys PW (2011) Optical coherence tomography (OCT) of overlapping bioresorbable scaffolds: from benchwork to clinical application. EuroIntervention 7(3):386–399. https://doi.org/10.4244/eijv7i3a64
39. Costa JR, Abizaid A, Bartorelli AL, Whitbourn R, Serruys PW, Smits PC (2017) Two-year clinical outcomes of patients treated with overlapping absorb scaffolds: an analysis of the ABSORB EXTEND single-arm study. Catheter Cardiovasc Interv. https://doi.org/10.1002/ccd.27223
40. Ortega-Paz L, Capodanno D, Giacchi G, Gori T, Nef H, Latib A, Caramanno G, Di Mario C, Naber C, Lesiak M, Capranzano P, Wiebe J, Mehilli J, Araszkiewicz A, Pyxaras S, Mattesini A, Geraci S, Naganuma T, Colombo A, Münzel T, Sabaté M, Tamburino C, Brugaletta S (2016) Impact of overlapping on 1-year clinical outcomes in patients undergoing everolimus-eluting bioresorbable scaffolds implantation in routine clinical practice: Insights from the European multicenter GHOST-EU registry. Catheter Cardiovasc Interv 89(5):812–818. https://doi.org/10.1002/ccd.26674
41. Tarantini G, Mojoli M, Masiero G, Cortese B, Loi B, Varricchio A, Gabrielli G, Durante A, Pasquetto G, Calabrò P, Gistri R, Tumminello G, Misuraca L, Pisano F, Ielasi A, Mazzarotto P, Coscarelli S, Lucci V, Moretti L, Nicolino A, Colombo A, Olivari Z, Fineschi M, Piraino D, Piatti L, Canosi U, Tellaroli P, Corrado D, Rovera C, Steffenino G (2017) Clinical outcomes of overlapping versus non-overlapping everolimus-eluting absorb bioresorbable vascular scaffolds: an analysis from the multicentre prospective RAI registry. Catheter Cardiovasc Interv. https://doi.org/10.1002/ccd.27095
42. Bangalore S, Bezerra HG, Rizik DG, Armstrong EJ, Samuels B, Naidu SS, Grines CL, Foster MT, Choi JW, Bertolet BD, Shah AP, Torguson R, Avula SB, Wang JC, Zidar JP, Maksoud A, Kalyanasundaram A, Yakubov SJ, Chehab BM, Spaedy AJ, Potluri SP, Caputo RP, Kondur A, Merritt RF, Kaki A, Quesada R, Parikh MA, Toma C, Matar F, DeGregorio J, Nicholson W, Batchelor W, Gollapudi R, Korngold E, Sumar R, Chrysant GS, Li J, Gordon JB, Dave RM, Attizzani GF, Stys TP, Gigliotti OS, Murphy BE, Ellis SG, Waksman R (2017) The state of the absorb bioresorbable scaffold: consensus from an expert panel. JACC Cardiovasc Interv 10(23):2349–2359. https://doi.org/10.1016/j.jcin.2017.09.041